

Elimination of the Voltage Oscillation Influence in the 3-Level VSI Drive Using Sliding Mode Control Technique

UDK 621.313.33.072.2
IFAC 5.5.4; 4.3.1

Original scientific paper

Today the three-level voltage-source inverters (3LVSI) are active used in the AC drive thanks to their merits as output signal quality improvements and a lower common mode voltage for semiconductor switches. However, their increased control complexity is the main barrier on the way to their extensive use. The cause is from one side a non-linear feature of control plant that is a series coupling of two non-linear objects: a switched converter and AC motor, and from another one a big set of 3LVSI output voltages. The sliding mode control (SMC) is one of the possible control solutions that gives the possibilities to design AC drive with the high dynamic feature in combination with robustness against disturbances and plant parameter variations. SMC does feasible overcoming one of the main problems of 3LVSI, namely the lower-frequency voltage oscillations that appear in the input DC-line voltage after the rectification of the industrial three-phase voltage and in the neutral point under some operating conditions. SMC based on the two-step control design procedure that takes into account the operation features of 3LVSI is designed. The original control algorithm includes a choice condition for 3LVSI input DC-line voltage and a switch table for the 3LVSI semiconductor switches. In its frame a choice condition for the input DC-line voltage based on the boundary conditions of both voltage oscillations is obtained. The performance of the considered control structure has been examined by simulation.

Key words: Induction motor drive, Three-level voltage source inverter, Sliding mode control, Voltage oscillation

Uklanjanje utjecaja oscilacija napona u trirazinskom učinskom pretvaraču s naponskim ulazom primenom kliznog načina upravljanja. Danas se za upravljanje izmjeničnim elektromotornim pogonima koriste trirazinski učinski pretvarači s naponskim ulazom, zbog njihovih svojstava kao što su poboljšanje harmonijskog sastava izlaznog napona i manje naponsko opterećenje učinskih sklopki pretvarača. Glavna prepreka široj uporabi trirazinskih učinskih pretvarača su složeni zahtjevi na upravljanje koji proizlaze iz nelinearnosti sustava koji je serijski spoj učinskog pretvarača i izmjeničnog stroja, te iz velikog broja stanja izlaznog napona trirazinskog učinskog pretvarača s naponskim ulazom. Klizni način rada je jedno od mogućih rješenja za upravljanje koje daje mogućnost projektiranja izmjeničnog elektromotornog pogona s izvrsnim dinamičkim svojstvima i robusnošću na promjene parametara sustava. Klizni način upravljanja uspješno rješava glavni problem trirazinskih učinskih pretvarača s naponskim ulazom – niskofrekvencijsku valovitost ulaznog istosmjernog napona dobivenog ispravljanjem industrijskog trofaznog izmjeničnog napona. Projektiran je klizni način upravljanja koji uzima u obzir svojstva trirazinskog učinskog pretvarača s naponskim ulazom. Izvorni upravljački algoritam obuhvaća izbor uvjeta za ulazni istosmjerni napon trirazinskog učinskog pretvarača s naponskim ulazom i tablicu sklopnih stanja učinskih sklopki trirazinskog učinskog pretvarača s naponskim ulazom. Ponašanje predložene upravljačke strukture ispitano je simulacijski.

Ključne riječi: asinkroni elektromotorni pogon, trirazinski učinski pretvarač s naponskim ulazom, klizni način rada, valovitost napona

1 INTRODUCTION

The multilevel converters, compared with conventional two level ones, offer additional benefits such as output signal quality improvements and a lower common mode voltage for semiconductor switches. These advantages made them very successful in the past decade, applied to the high and medium voltage drive field, and, especially, the neutral point (NP) clamped three-level voltage-source invert-

ers (3LVSI) equipped by power semiconductor switches [1, 2].

Despite all their advantages, these converters are not widely used, and the main reason is their increased control complexity. It connects with the set of the variable structures of 3LVSI that depend on the position combination of the switches. The alternating current (AC) drive is a non-linear control plant having a series coupling of

two non-linear objects, which are different by nature, i.e. a switched converter and AC motor [3]. There are different machine models depending on the reference frame and the space variables. As a consequence, a large number of the control methods have been proposed, but nearly all these techniques have in common the decomposition of the main high-order task of the drive control design to several separated lower-order tasks. One of them is the 3LVSI control design, solved by using different types of PWM [1, 2]. As all feed forward controls this one is sensitive to control parameters changes and plant disturbances, such as a DC-link voltage change. In addition, a NP voltage oscillation can appear under some operating conditions. A great deal of research has been focused on this field [4].

From another side the switching nature of 3LVSI opens the possibility to use the principal operational mode for this class of control systems – sliding mode control (SMC) – to solve the control task. It is well known that one of the main advantages of SMC is the control system robustness against disturbances and plant parameter variations by a very high dynamic and accuracy. Many different control solutions for the drives with classical two-level voltage source inverter based on SMC were proposed [5–11]. SMC strategy for induction motor (IM) drive with 3LVSI is proposed in [12]. The control design is based on a two-step control design procedure. The nonlinearities of IM and 3LVSI are taken separately into account in this approach. The control algorithm designed originally includes a choice condition for the 3LVSI DC-link voltage and a switch table for the 3LVSI semiconductor switches, which connects the switch controls with the signs of the control variables errors according to the AC motor angle position.

The primary aim of this paper is to show that in the frame of the above-mentioned SMC algorithm the robustness against DC-link voltage change and NP voltage oscillation could be guaranteed. The paper is outlined as follows. At the beginning (Section 2) briefly the employed models of IM and 3LVSI are presented and discussed. Then (Section 3) the SMC design on the base of the two-steps technique for the control synthesis is presented. Its three subsections describe the selection of the SMC functions, the classical SMC design in the stator-flux-rotating frame and the designed control transformation into the 3LVSI switch controls. As design result the SMC algorithms are obtained. In Section 4 the proposed SMC algorithm is investigated from the viewpoint of the robustness guarantee against a DC-link voltage change and a NP voltage oscillation and a choice condition for the input DC-line voltage is obtained. Section 5 presents the results of the numerical simulation examination that illustrate the properties of the suggested SMC. Section 6 concludes the paper. The appendix contains a brief introduction into SMC design backgrounds.

2 USED MATHEMATIC MODELS

As known [13] the drive is an electromechanical converter that transforms the input electrical power in the output mechanical one. From the power viewpoint it has two parts: a power transformer and a control. The power part has a serious coupling of two non-linear objects: 3LVSI and IM. Its inputs are the controls of the 3LVSI switches and its output is the mechanical coordinate of IM, e.g. rotor angle position or speed or electromagnetic torque. The transformation of the electrical power in the mechanical one directly results in IM. However in the frame of the power part 3LVSI controls this process, as it controls the IM phase voltages. The control controls the power part and realizes the needed power transformation algorithm, e.g. the needed mechanical coordinate control. The control structure depends on the structure of the power part and its possible controls. Below from the control viewpoint the used mathematical descriptions are presented that are used by the control design.

2.1 Three level voltage source inverter

As shown in Fig. 1 the topology feature of the NP clamped 3LVSI is a capacitor voltage divider that produces a NP potential (M) [14]. There are three input potentials here: the positive (L+) one and the negative (L-) one of the dc-link voltage V_{dc} and the middle potential between positive and negative potential (M). For the proper operation of 3LVSI, the NP voltage must be kept at one half of the DC-link voltage ($v_{C_1} = v_{C_2} = V_{dc}/2$). Under such condition the output voltage space vector can have 19 different values by using all possible position combinations of the three-position semiconductor switches (S1, S2, S3). They are presented in Fig. 2 near the vector positions, where “+” means it is connected with L+; “-” with L-; and “0”, with M. There are four vector groups:

1. six full-voltage space vectors (A) with magnitude $B_A = \frac{V_{dc}}{3}$;
2. six intermediate-voltage space vectors (Z) with magnitude $B_Z = \frac{\sqrt{3}V_{dc}}{3}$;
3. six half-voltage space vectors (H) with magnitude $B_H = \frac{V_{dc}}{3}$. Each one is achieved by two switch combinations (there is a redundancy, used commonly to balance the middle potential);
4. the zero-voltage vector (N) that has three possible switch combinations.

2.2 Induction motor

This is one of the classic models of a symmetrical balanced squirrel-cage IM that has been written in the stationary reference frame (α , β) and with rotor quantities

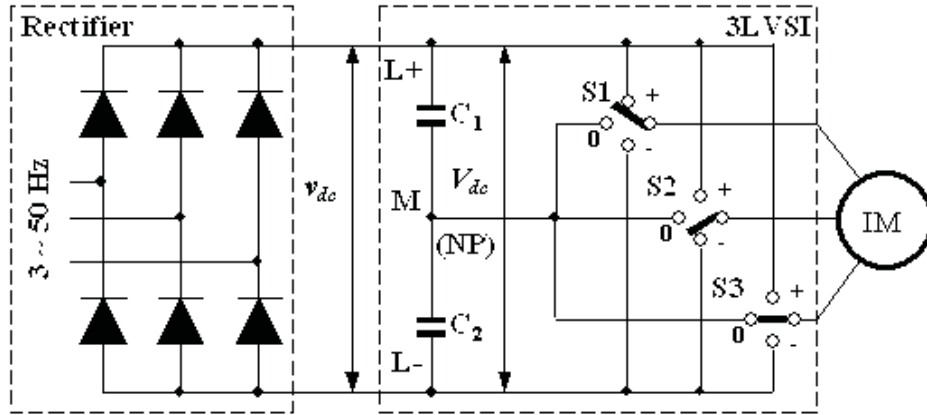


Fig. 1. Canonical schema of the drive power part with the NP-clamped 3L VSI

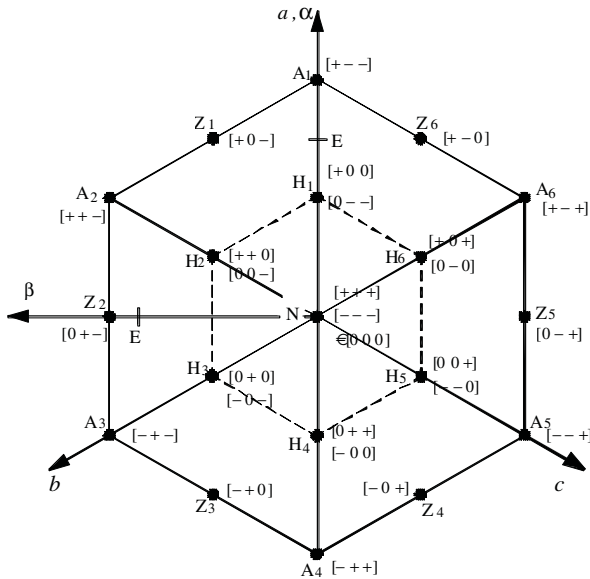


Fig. 2. 3L VSI voltage space-vector diagram

referred to stator [13]:

$$d(\omega/p)/dt = (T - T_L)/J, \quad (1a)$$

$$d\Psi_{s\alpha}/dt = -R_s i_{s\alpha} + u_{s\alpha}, \quad (1b)$$

$$d\Psi_{s\beta}/dt = -R_s i_{s\beta} + u_{s\beta}, \quad (1c)$$

$$di_{s\alpha}/dt = [R_r \Psi_{s\alpha}/(L_s L_r) + \omega \Psi_{s\beta}/L_s]/\sigma - \omega i_{s\beta} - \gamma i_{s\alpha}/L_s + u_{s\alpha}/L_s, \quad (1d)$$

$$di_{s\beta}/dt = [R_r \Psi_{s\beta}/(L_s L_r) + \omega \Psi_{s\alpha}/L_s]/\sigma + \omega i_{s\alpha} - \gamma i_{s\beta}/L_s + u_{s\beta}/L_s. \quad (1e)$$

Here ω is the electrical velocity; J is the inertia and T is the electromagnetic torque.

$$T = p(\Psi_{s\alpha} i_{s\beta} - \Psi_{s\beta} i_{s\alpha}), \quad (2)$$

T_L is the load torque; $\Psi_s^T = (\Psi_{s\alpha}, \Psi_{s\beta})$ is the stator flux vector; $i_s^T = (i_{s\alpha}, i_{s\beta})$ is the stator current vector; $u_s^T = (u_{s\alpha}, u_{s\beta})$ is the stator voltage vector; R and L denote resistance and self inductance, subscripts s and r stand for stator and rotor; p is the pole pair number; $\sigma = 1 - L_m^2/(L_s L_r)$, with L_m being the mutual inductance; $\gamma = \frac{L_s R_r}{L_r} - R_s$.

The stator current i_s and voltage u_s vectors are connected to the phase current $I_s^T = (i_a, i_b, i_c)$ and voltage $U_s^T = (u_a, u_b, u_c)$ ones using the transformation

$$i_s = C I_s, \quad u_s = C U_s, \quad (3)$$

where C is the transformation matrix,

$$C = \sqrt{2/3} \begin{bmatrix} 1 & -1/2 & -1/2 \\ 0 & \sqrt{3}/2 & -\sqrt{3}/2 \end{bmatrix}. \quad (4)$$

3 SLIDING MODE CONTROL DESIGN

3.1 Sliding mode functions selection

The main goal of the IM drive control is satisfied, if the average value of the mechanical output variable (e.g. a rotor speed or a position) will equal the set value, which has subscript z . In the case of the shown in Fig. 3 cascade control [13] this task is reduced to the task of maintaining the target torque T at the shaft of the motor. As the number of the independent controls is equal to the order of the control space, in the case of IM drive the voltage plane, and higher as one, it is first of all possible to control two variables: not only one mechanical variable, but another variable which

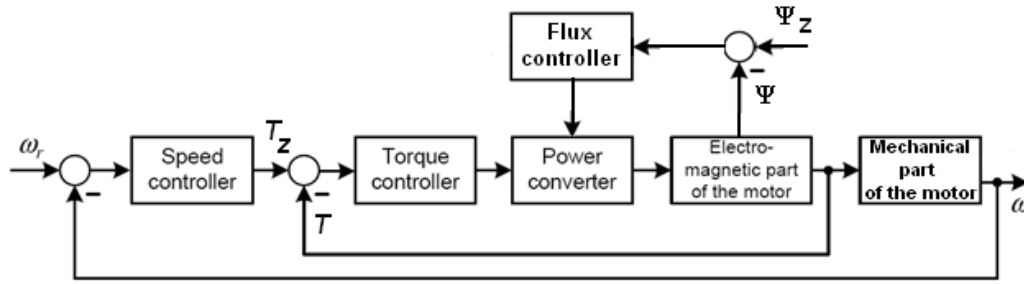


Fig. 3. Classical cascade control schema

describes electrical or power requirements of the IM. Usually the stator-flux modulus

$$|\Psi_s| = \sqrt{\Psi_{s\alpha}^2 + \Psi_{s\beta}^2} \quad (5)$$

is chosen. So, for the control design the error function F must be formed dimension of which is equal to the control dimension and the components representing the functions of control error that must be zero:

$$F = \begin{vmatrix} F_\Psi \\ F_T \end{vmatrix} = \begin{vmatrix} |\Psi_{sz}| - |\Psi_s| \\ T_z - T \end{vmatrix}. \quad (6)$$

One of the possible ways for doing this is the organization of a sliding motion on the manifold (6), (27).

3.2 Main idea of design technique

The proposed in [12] SMC for an IM drive supplied by 3LVSI allows organizing a sliding mode motion in the electromechanical system, where the number of the discontinuous controls is first of all bigger than the control order, and these controls are constant and cannot be changed. Only above-mentioned 19 different output voltage space vectors of 3LVSI can be used for solving the task of the SMC design for the IM drive. However its control space order is two.

The control design is based on two-step design technique [5, 6]. The main idea of this technique is the decomposition of the control task, taking into account separately the nonlinearities of IM and 3LVSI. At the first step only the two-phase equivalent model of the IM has been used. In this case the number of discontinuous controls is equal to the order of the voltage plane. The sliding mode can be designed by using the standard technique. At the second step the real discontinuous output voltages of 3LVSI have been taken into account, and the realization task of the above-mentioned sliding mode has to be solved with them. The switching law for the phase power switches that guaranties SMC have been designed.

3.3 Design in the stator-flux rotating frame

As stated above, the control aim is designing such control law that the state reaches the sliding manifold (6), (27), which is the same as the error function (6) being zero, in finite time from the bounded initial conditions, and then remain on it. In this case the control task has been fulfilled. For the solving of such control task the equation of the error function variation in the moving coordinate frame coupled with the stator-flux is used

$$\begin{aligned} \frac{d}{dt} \begin{vmatrix} F_\Psi \\ F_T \end{vmatrix} &= \\ & \begin{vmatrix} d|\Psi_{sz}|/dt + R_s(\Psi_{s\alpha}i_{s\alpha} + \Psi_{s\beta}i_{s\beta})/|\Psi_s| \\ dT_z/dt + (\gamma + \omega\Psi_s^2)/(\sigma L_s) - \omega(\Psi_{s\alpha}i_{s\alpha} + \Psi_{s\beta}i_{s\beta}) \end{vmatrix} - \\ & \begin{vmatrix} 1/|\Psi_s| & 0 \\ T/|\Psi_s| & |\Psi_s|/(\sigma L_s) + (\Psi_{s\alpha}i_{s\alpha} + \Psi_{s\beta}i_{s\beta})/|\Psi_s| \end{vmatrix} \times \\ & \times \begin{vmatrix} \cos \rho & \sin \rho \\ -\sin \rho & \cos \rho \end{vmatrix} \times \begin{vmatrix} u_{s\alpha} \\ u_{s\beta} \end{vmatrix}, \end{aligned} \quad (7)$$

where $\rho = \arctan(\psi_{s\beta}/\psi_{s\alpha})$ is the stator-flux angle.

Although the transformation from (1) to (7) is not defined for zero flux, this limitation is not a critical concern for the IM control. Usually the flux is initialized to a nonzero value.

One of the features of (7) is a matrix with the periodical coefficients before the stator voltage vector that makes the control task solving more complicated. For control design simplification the new control vector connected to the control vector u_s using the transformation

$$\begin{vmatrix} u_{s\alpha} \\ u_{s\beta} \end{vmatrix} = \begin{vmatrix} \cos \rho & -\sin \rho \\ \sin \rho & \cos \rho \end{vmatrix} \times \begin{vmatrix} u_\psi \\ u_T \end{vmatrix}, \quad (8)$$

is suggested to be used.

By using such control the matrix before the new control vector have not the periodical coefficients, and the sliding motion on the manifold can be designed using the control hierarchy method [7], because the error function F_Ψ depends only on control u_ψ . In this case the problem of sliding domain is reduced to a sequential analysis of two scalar

cases. The scalar sliding mode condition is

$$\lim_{F \rightarrow 0^+} (dF/dt) < 0 \ \& \ \lim_{F \rightarrow 0^-} (dF/dt) > 0. \quad (9)$$

The control vector components u_Ψ and u_T are selected depending upon the sign of the components of the error function F :

$$u_\Psi = U_\Psi \operatorname{sgn} F_\Psi, \quad (10)$$

$$u_T = U_T \operatorname{sgn} F_T. \quad (11)$$

Their magnitudes U_Ψ and U_T can be selected using the inequalities

$$U_\Psi \geq U_{\Psi eq} = \left| |\Psi_s| \frac{d|\Psi_{sz}|}{dt} + R_s (\Psi_{s\alpha} i_{s\alpha} + \Psi_{s\beta} i_{s\beta}) \right|, \quad (12)$$

$$U_T \geq U_{T eq} = \left| \frac{dT_z}{dt} - \frac{T}{|\Psi_{sz}|} \times \frac{d|\Psi_{sz}|}{dt} + \frac{1}{\sigma} \left(\frac{\gamma}{L_s} + \frac{p}{L_s} \omega \Psi_s^2 \right) - \left(p\omega + \frac{R_s T}{\Psi_{sz}^2} \right) (\Psi_{sa} i_{sa} + \Psi_{sb} i_{sb}) \right|, \quad (13)$$

where $U_{\Psi eq}$, $U_{T eq}$ are the equivalent controls (30).

The equivalent control is a continuous control that would guarantee the same motion, if all needed information about the load and the system uncertainty were available. In this case the system behavior can be written with a vector equation of reduced order. The full order is reduced to the order of the sliding-mode manifolds.

The magnitudes U_Ψ and U_T bound the initial condition, from which the state will reach the sliding manifold in finite time, and the uncertainty of the system and the load value to that the system is robust in general.

The approach to the design of the switch control is based on the fact that the choice conditions of the amplitudes of the formally entered controls in the stator-flux rotating frame bases on the inequalities (12) and (13). In this case there is an area of allowable controls U^* in the space of the formally entered controls u_Ψ , u_T that guarantee sliding motion: $U^* = \{U^*\} = U_1^* \cup U_2^* \cup U_3^* \cup U_4^*$, $U_1^* \cap U_2^* = 0$, $U_1^* \cap U_3^* = 0$, $U_1^* \cap U_4^* = 0$, $U_2^* \cap U_3^* = 0$, $U_2^* \cap U_4^* = 0$, $U_3^* \cap U_4^* = 0$, each subarea U_i^* , $i = 1, \dots, 4$ has its combination of the controls $\operatorname{sgn} F_T$ and $\operatorname{sgn} F_\Psi$. Table 1 shows the connection between these subareas and the combination of the controls $\operatorname{sgn} F_T$ and $\operatorname{sgn} F_\Psi$.

Table 1. Control subareas in the stator-flux rotating frame

	U_1^*	U_2^*	U_3^*	U_4^*
$\operatorname{sgn} F_\Psi$	1	-1	-1	1
$\operatorname{sgn} F_T$	1	1	-1	-1

3.4 Design of controls for the semiconductor switches

In reality, as shown in the subsection 2.1 there are only 19 different output voltage space vectors with four different magnitudes, produced by discontinuous control (switching) of the balanced 3LVSI. The question is whether it is possible to attain the above designed sliding motion with these output vectors. Of course, one of the possible ways is to use the inverse to (6) transformation and to generate three-phase voltage references by using the feed-forward PWM. The sine-wave voltages would be the mean values of the output voltages of the semiconductor 3LVSI with high-frequency switches. However the realization of PWM need additional information such, as the average value of the output voltage space vector U_{eq} during any time period, the switching time for each switch and the sequence of their switching that must be calculated. Such approach requires additional calculations and does not reach any of the basic properties of sliding mode, namely simplicity of realization, insensitivity to parameter variations and to a load.

The alternative approach to design of 3LVSI output voltages control, i.e. transferring the two-dimensional control (10)–(13) to the 3LVSI switch control, is based on the fact, that the selection conditions of the amplitudes of the formally entered controls in the reference frame rotating with stator-flux use the inequalities (12) and (13). In this case there is an area of allowable controls U^* in the space of the formally entered control shown in Fig. 4. Obviously, if we design the real discontinuous voltages such that their projections on suitable axes of the stator-flux-rotating frame have their marks and sizes, which are needed by the control algorithm with the formally entered controls, the sliding mode on crossing before the chosen surfaces will take place. Of course, the sizes of the formally entered control values will change during operation.

The sliding mode, which has been synthesized in the stator-flux rotating frame, can be secured by using the discontinuous voltages of the 3LVSI, if each control area has at any time at minimum one of the 3LVSI output voltage vectors. Fulfilling this condition it is necessary to calculate the 3LVSI input voltage and to design a transition law between the designed control (12), (13) and the switching control of 3LVSI switches. By the below mentioned control design procedure the following assumptions were used:

- the used 3LVSI output-voltage space vectors are full ones and intermediate ones;
- the value of the 3LVSI dc-link voltage must be the minimal possible;
- the selected values of the magnitudes U_Ψ and U_T are equal to U_0 .

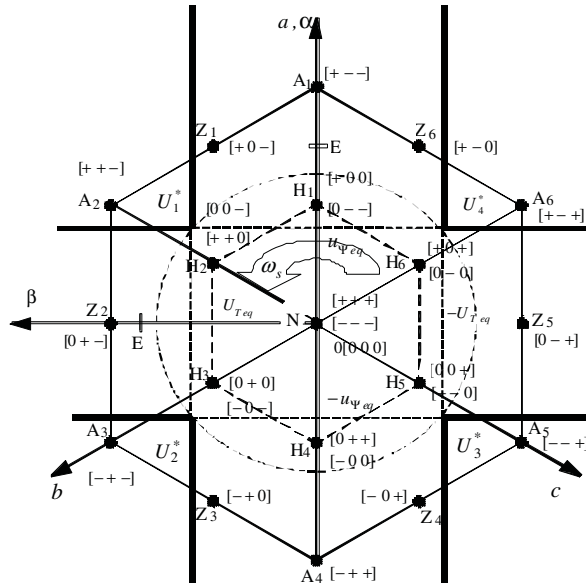


Fig. 4. Sliding mode control areas and voltage space-vector of 3LVSI

- the value of the 3LVSI dc-link voltage was calculated using the magnitude of the intermediate voltage space vectors, i.e. there is the supply voltage $B_A - B_Z = (2 - \sqrt{3})V_{dc}/3$.

In this case the selection condition of the 3LVSI input DC-voltage value, for geometrical reasons, is

$$\arcsin(U_0/B_z) \leq \pi/6 \quad (14)$$

and the 3LVSI DC-link voltage value can be calculated as

$$V_{dc} \geq V_{dc \min} = 2\sqrt{3} \cdot U_0. \quad (15)$$

This 3LVSI DC-link voltage value guarantees that the sliding motion designed on the first step will be executed by the above mentioned 3LVSI output voltage space vectors, i.e. the system will reach the sliding manifold from initial condition selected in the first design step in finite time and remain on it and will be robust against the selected uncertainty of the system and the load value accordance the inequalities (12), (13).

The transfer strategy from the controls $\text{sgn}F_T$ and $\text{sgn}F_\Psi$ to control S_a, S_b, S_c of the switches S1, S2 and S3 is presented in Tab. 2 and Tab. 3. There are 12 equal stator-flux-angle zones of size $\pi/6$, where switch control is equal to one of the controls $\text{sgn}F_T$ and $\text{sgn}F_\Psi$ or their opposite values.

Table 2. Phase switches controls

ρ	S_a	S_b	S_c
$(0 \dots \pi/6)$	$\text{sgn}F_\Psi$	$\text{sgn}F_T$	C
$(\pi/6 \dots \pi/3)$	D	$\text{sgn}F_T$	$-\text{sgn}F_\Psi$
$(\pi/3 \dots \pi/2)$	$-\text{sgn}F_T$	A	$-\text{sgn}F_\Psi$
$(\pi/2 \dots 2\pi/3)$	$-\text{sgn}F_T$	$\text{sgn}F_\Psi$	B
$(2\pi/3 \dots 5\pi/6)$	C	$\text{sgn}F_\Psi$	$\text{sgn}F_T$
$(5\pi/6 \dots \pi)$	$-\text{sgn}F_\Psi$	D	$\text{sgn}F_T$
$(\pi \dots 7\pi/6)$	$-\text{sgn}F_\Psi$	$-\text{sgn}F_T$	A
$(7\pi/6 \dots 4\pi/3)$	B	$-\text{sgn}F_T$	$\text{sgn}F_\Psi$
$(4\pi/3 \dots 3\pi/2)$	$\text{sgn}F_T$	C	$\text{sgn}F_\Psi$
$(3\pi/2 \dots 5\pi/3)$	$\text{sgn}F_T$	$-\text{sgn}F_\Psi$	D
$(5\pi/3 \dots 11\pi/6)$	A	$-\text{sgn}F_\Psi$	$-\text{sgn}F_T$
$(11\pi/6 \dots 2\pi)$	$\text{sgn}F_\Psi$	B	$-\text{sgn}F_T$

Table 3. Quantities A, B, C and D for Tab. 2

$\text{sgn}F_\Psi$	1	1	-1	-1
$\text{sgn}F_T$	1	-1	1	-1
A	1	0	0	-1
B	0	-1	1	0
C	-1	0	0	1
D	0	1	-1	0

This 3LVSI DC-link voltage value (15) and control Tab. 2 and 3 guarantee that the system will in finite time reach the sliding manifold (6), (27) from initial condition selected in (12), (13), will remain on it and will be robust with respect to the selected uncertainty of the system parameters.

As the design result, the SMC algorithms (6), (10)-(13), (15), Tab. 2 and Tab. 3 are obtained that guarantee zero torque and flux-modulus errors by variation of drive parameters, load and inverter DC-link voltage.

4 ROBUSTNESS AGAINST VOLTAGE OSCILLATION

4.1 NP voltage oscillation

The voltages on the capacitors are changed by using the NP voltage for producing the output voltage space vector. In this case the intermediate voltage space vectors oscillate near their rated position suitable to the mode with the balanced NP voltage presented in Fig. 2.

Figure 5 shows an oscillation area of the vector Z_1 . On the symmetry strength another intermediate-voltage vectors have the same behavior. The angle motion of the space vector is bounded.

$$|\xi| \leq \Xi, \quad (16)$$

where: $|\xi|$ is actual angle deviation, and Ξ is the maximal one.

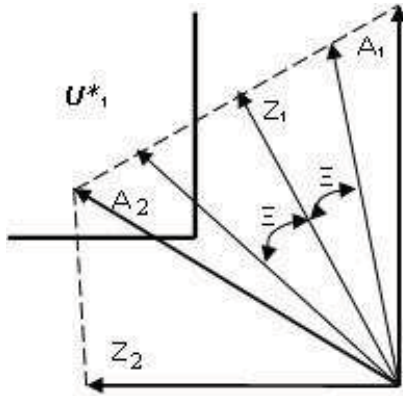


Fig. 5. Oscillation area of the intermediate-voltage vector Z_1

The SMC will be secured by the misbalance of the NP voltage, if each control area has at any time at minimum one of the 3LVSI output voltage vectors. This condition is fulfilled by using the logical switch control table and by calculating the DC-line voltage subject to the maximal angle deviation Ξ . The selection condition of the input DC-link voltage value, for geometrical reasons, is

$$\arcsin(U_0/B_z^*) \leq \pi/6 - \Xi/2, \quad (17)$$

where B_z^* is the magnitude of the intermediate-voltage space vector that corresponds to the maximal angle deviation Ξ :

$$B_z^* = B_z / \cos \Xi. \quad (18)$$

The 3LVSI DC-link voltage value, by using (18), can be calculated as:

$$V_{dc} \geq V_{dc \min} = (\sqrt{3} \cdot U_0) \cos \Xi / [\sin(\pi/6 - \Xi/2)]. \quad (19)$$

In case DC-link voltage used satisfies relation (19), the drive robustness against the NP voltage oscillation is guaranteed.

4.2 DC-link voltage changes

In fact the DC-link voltage is usually produced from three-phase AC voltages by using three-phase, six-pulse, full bridge diode rectifier with a filter capacitor in the DC-link (Fig. 1). The purpose of this capacitor is to eliminate the ripple from the DC output voltage from the rectifier, as much as possible (Fig. 6). In this case the DC-link voltage is:

$$V_{dc} = \frac{3}{\pi} \int_{-\infty}^{\infty} \sqrt{2} V_{LL} \cos(\omega_l f t) d(\omega_l f t) = 1,35 V_{LL}, \quad (20)$$

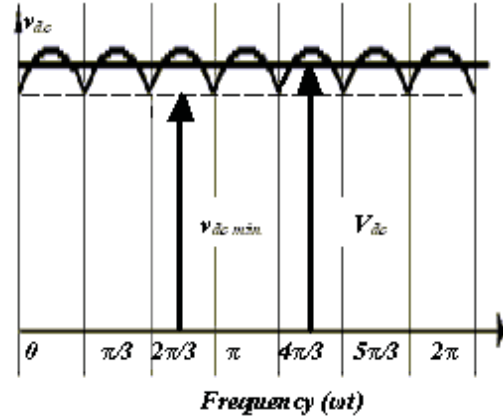


Fig. 6. Waveform of the rectifier DC-side voltage v_{dc} and the DC-link voltage V_{dc}

where V_{LL} is the rms value of the line to line voltage, $\omega_l f$ is a line frequency, t is time.

The instantaneous waveform of the rectifier DC-side voltage v_{dc} consists of six segments per cycle of line frequency. The minimal value of this voltage $v_{dc \min}$ is

$$v_{dc \min} = \sqrt{6} V_{LL} / 2 = 1.22 V_{LL}. \quad (21)$$

As a selection condition for the input DC-link voltage value is an inequality, the sliding motion could be guaranteed by changing the rectifier DC-side voltage v_{dc} . Only its lowest value must be bounded, i.e.

$$v_{dc \min} \geq 2\sqrt{3} \cdot U_0. \quad (22)$$

It is possible in this case to reduce the value and therefore the size of the filter capacitor.

If one wants to have the robustness to both voltage oscillations, so NP one and DC-line one, the lowest value of the DC-link voltage must be calculated using (19) as

$$v_{dc \min} \geq (\sqrt{3} \cdot U_0) \cos \Xi / [\sin(\pi/6 - \Xi/2)]. \quad (23)$$

5 FIRST SIMULATION RESULTS

To exemplify the behaviour of the IM drive with sliding-mode controller simulations were performed for IM and 3LVSI taken from [2]. The underlying IM parameters are shown in Table 4.

The DC-link voltage of the 3LVSI is $V_{dc} = 422$ V, the control cycle time is $25 \mu s$. The 3LVSI state was determined by the sliding-mode controller that uses as input signals the error signs (10), (11) and information about the stator-flux position and produces the output signals, using Tab. 2 and Tab. 3.

Parameter	Symbol	Value
Rated power (kW)	P_r	90
Rated voltage (V)	U_r	330
Rated current (A)	I_r	180
Number of pole pairs	p	2
Rated speed (rpm)	n_r	1480
Rated torque (Nm)	T_r	1160
Rated flux linkage amplitude (Wb)	Ψ	1.71
Stator resistance (mΩ)	R_s	25.9
Rotor resistance (mΩ)	R_r	18
Magnetizing inductance (mH)	L_μ	27.6
Leakage inductance (mH)	L_σ	1.3

Table 4. Parameters of IM for simulation

In a first step, the design of the sliding-mode controller uses only the full and intermediate voltage space-vectors. Speed was thus held constant at 82% of rated speed, 1200 rpm, which is appropriate, using only these space vectors. All quantities (except time) are given in p.u., with the flux normalized to rated stator-flux amplitude (1.71 Wb), torque to rated break-down torque $T_b = 3373$ Nm, rated torque being 35% of break-down torque. Currents are normalized to the rated ideal rotor short-circuit current $I_\infty = \Phi_z/L_\sigma = 1315$ A and voltages to $2/\pi \cdot V_{dc} = 368$ V.

The flux and torque hysteresis bands were set to 7% of rated flux amplitude and break-down torque, respectively. The resulting device switching frequency is below 300 Hz.

Figure 7 and Fig. 8 show the drive start. At $t = 0$ the machine is magnetized to rated flux, at $t = 0.5$ s the torque set value is raised to 35% of break-down torque. Figure 9 and Fig. 10 present the torque reducing to 20% of break-down torque at $t = 0.7$ s.

Figure 8 and Fig. 10 display the time functions of torque

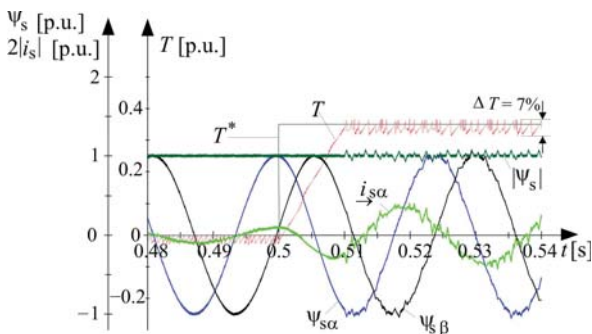


Fig. 7. Torque T and torque set value T^* , α , β components of stator-flux space vector $\Psi_{s\alpha}$, $\Psi_{s\beta}$ and modulus $|\Psi_s|$, stator current $i_{s\alpha}$ with the modulus $2|i_s|$; torque set value rising from 0 to 35% T_b of the rectifier dc-side voltage v_{dc} and the dc-link voltage V_{dc}

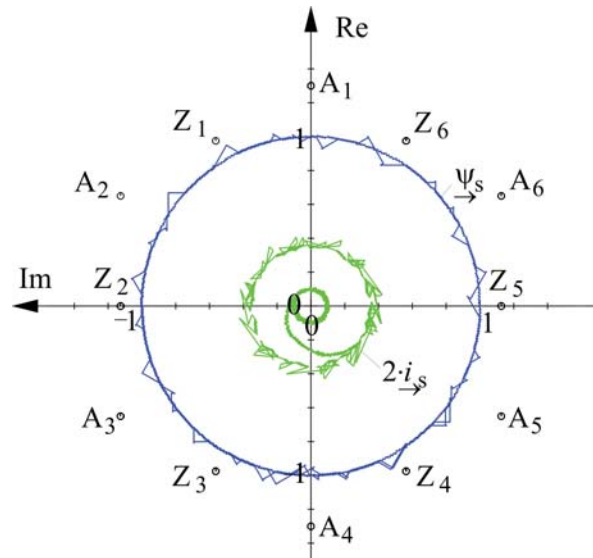


Fig. 8. Space-vector trajectories of stator flux Ψ_s , stator current $i_{s\alpha}$ with the modulus $2|i_s|$ and stator voltage, torque set value rising from 0 to 35% T_b

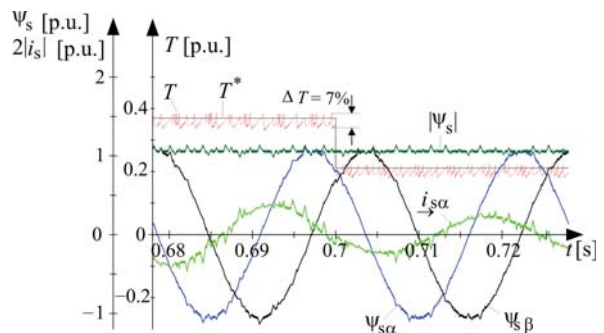


Fig. 9. Torque T and torque set value T^* , α , β components of stator-flux space vector $\Psi_{s\alpha}$, $\Psi_{s\beta}$ and modulus $|\Psi_s|$, stator current $i_{s\alpha}$ with the modulus $2|i_s|$; torque set value reduced from 35% T_b to 20%

and torque set value, the α - and β -coordinates of the stator-flux space vector $\Psi_{s\alpha}$, $\Psi_{s\beta}$ and its modulus $|\Psi_s|$ and the (double of the) α -coordinate of the stator-current space vector is $i_{s\alpha}$ (current in phase a). The torque rise is achieved – due to the reduced voltage margin – only within 10.2 ms, but the torque reduction shows the dynamics to be expected from direct control, with a sink time of 0.12 ms approximately. Torque and flux modulus are guided safely in their bands, the flux and current waveforms are mainly sinusoidal, with small distortions.

Figure 7 and Fig. 9 show the trajectories of the space vectors of stator flux Ψ_s , the double of the stator current

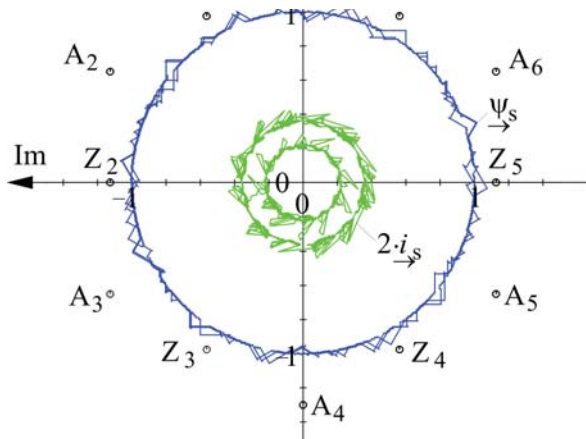


Fig. 10. Space-vector trajectories of stator flux Ψ_s , stator current $i_{s\alpha}$ with the modulus $2|i_s|$ and stator voltage, torque set value reduced from 35 to 20% T_b

i_s and the employed full (A) and intermediate (Z) voltage states, belonging to Fig. 8 and Fig. 10.

The pertaining fundamental current amplitudes (= radii of trajectories) $i_{s0} = \sigma/(1-\sigma)I_\infty$ are:
 no load: $i_{s0} = 0.047I_\infty$;
 rated load ($T = 0.35T_b$): $i_{s0} = 0.19I_\infty$;
 57% rated load ($T = 0.2T_b$): $i_{s0} = 0.12I_\infty$.

6 CONCLUSION

The application of this sliding-mode technique to the control design of an AC drive supplied by a 3LVSI allows elimination of the influences of the NP voltage oscillations and DC-link voltage changes in the drive behavior. The selection conditions for the choice of the DC-link voltage value in the frame of the SMC algorithm are proposed [12]. The designed drive control would be able to guarantee all advantageous characteristics of the control plant. Such type of the control is a very high dynamic one and has a very low sensitivity to disturbances, caused both by the load, the input DC-link voltage and plant parameter variations.

The next improvement of the torque control performance is to use half-voltage and zero-voltage space vectors by proper design of the controller.

APPENDIX A SLIDING MODE BACKGROUNDS

The control design in this paper is based on sliding mode as a special type of behavior of a relay system [7]:

$$dx(t)/dt = l(x, t) + B(x, t)u(t), \quad (24)$$

$$u_i(x, t) = \begin{cases} u_i^+(x, t) & \text{if } S_i(x, t) > 0, \\ u_i^-(x, t) & \text{if } S_i(x, t) < 0, \end{cases} \quad (25)$$

where $x(t)$ is a state vector, $x(t) \in \mathbb{R}^n$; $l(x, t)$ is a system vector, $l(x, t) \in \mathbb{R}^n$; $u(t)$ is a control vector, $u(t) \in \mathbb{R}^m$, $n \geq m$; $u_i(t)$ is a component of the control vector $u(t)$, $i = 1, \dots, m$; $B(x, t)$ is a matrix, $B(x, t) \in \mathbb{R}^{n \times m}$; $S_i(t)$ is a switching function.

The main feature of this mode is that none of the used general switched structures can realize such behavior. The sliding mode occurs in the intersection of all m surfaces

$$f_i = 0 \quad (26)$$

by using a switching of the control components $u_i(x, t)$ (25) with high frequency. The vector function $F^T = (f_1, \dots, f_m)$ is a function of the system variables $x(t)$ and is usually an error function that must be led to zero by using the vector switching function $S^T = (S_1, \dots, S_m)$.

Formally, the control aim is the following: the system state $x(t)$ must come to the manifold

$$F = 0 \quad (27)$$

and “slides” on this manifold to the reference point, independently of the system dynamic.

In this case the control design procedure is decoupled into two tasks:

- sliding mode design in the space of the vector function $F \in \mathbb{R}^m$;
- motion design on the intersection of all m surfaces in the state space with order $(n - m)$.

The solution of the first task solution is based on the Lyapunov stability of the control plant in the space of the vector function $F \in \mathbb{R}^m$. A typical sliding mode control u has the form

$$u = -U(x) \text{sgn}(F), \quad (28)$$

where $U(x)$ is the square diagonal matrix of the control magnitude; $\text{sgn}(F)$ is the vector of the signs of the error functions, $[\text{sgn}(F)]^T = (\text{sgn}f_1, \dots, \text{sgn}f_m)$. It guarantees that the system state will reach the sliding manifold in finite time from the initial condition, which has been bounded by the value of the constituent of the matrix $U(x)$, and will keep to it. This magnitude bounds the uncertainty of the system, the load value with respect to which the system is commonly robust. The special task is a design of a transition law between the designed control (28) and the switching control (25). It depends on the features of the relay system (24).

The motion on the sliding manifold is described by using the equivalent control $u_{eq}(x)$. It is calculated from the

condition that the time-derivative of the function F on the system trajectories is equal to zero

$$dF/dt = Gl + GBu_{eq} = 0, \quad (29)$$

where $G(x) = \{\partial F/\partial x\}$, $G(x) \in R^{m \times n}$ is a gradient matrix; $\det GB \neq 0$.

In this case the equivalent control $u_{eq}(x)$ that is a continuous control that would guarantee the same motion, if all needed information about the load and the system uncertainty were available, is calculated

$$u_{eq} = (GB)^{-1}Gl, \quad (30)$$

and the system motion in the sliding mode is described as

$$dx/dt = l - B(GB)^{-1}Gl \quad (31)$$

together with (28). Using (28) the system order can be reduced to $(n - m)$, and the system description is

$$dx_1/dt = l_1[x_1, t], \quad (32)$$

where $x^T = (x_1, x_2)$, $x_1 \in R^{n-m}$, $x_2 \in R^m$; $l_1[x_1, t]$, $l_1 \in R^{n-m}$.

ACKNOWLEDGMENT

The author wishes to acknowledge the support from the German Academic Exchange Service through research grant "Study visit of foreign academic personnel to the Federal Republic of Germany" (A/06/27385) that gave a start for this research. Many thanks on the placecountry-regionGermany colleagues from the Institute for Electrical Power Engineering and Power Electronics, Ruhr-University Bochum Prof. Andreas Steimel and Richard Schmidt-Obermoeller, together with whom the first steps in this research direction have been done. The author is very thankful to the EDPE session chairman Prof. Asif Šabanović for his good rating of the presented scientific results. Furthermore, the authors wish to thank his friends from Zagreb University Prof. Drago Ban, Prof. Željko Jakopović (EDPE 2009 General Chair) and Prof. Nedjeljko Perić (KoREMA President) for their help with participation in such famous scientific event as EDPE 2009. Finally, many thanks to all colleagues who supported this research.

REFERENCES

- [1] J. Rodriguez, S. Bernet, B. Wu, J. O. Pontt, and S. Kouro, "Multilevel voltage-source-converter topologies for industrial medium-voltage drives," *IEEE Transactions on Industrial Electronics*, vol. 54, no. 6, pp. 2930–2945, 2007.
- [2] E. Krafft, A. Steimel, and J. K. Steinke, "Three-level high-power inverters with IGCT and IGBT elements compared on the basis of measurements of the device losses," in *Proceedings of 8th European Conference on Power Electronics EPE'99*, (Lausanne, Switzerland), 1999.
- [3] Z. Suto and I. Nagy, "Nonlinearity in controlled electric drives: Review," in *Proceedings of 2006 IEEE International Symposium on Industrial Electronics*, (Montreal, Canada), pp. 2069–2076, 2006.
- [4] J. Pou, J. Zaragoza, P. Rodriguez, S. Ceballos, V. M. Sala, R. P. Burgos, and D. Boroyevich, "Fast-processing modulation strategy for the neutral-point-clamped converter with total elimination of low-frequency voltage oscillations in the neutral point," *IEEE Transactions on Industrial Electronics*, vol. 54, no. 4, pp. 2288–2294, 2007.
- [5] S. Ryvkin, "Sliding mode technique for ac drive," in *Proceedings of the 10th International Power Electronics & Motion Control Conference (EPE-PEMC 2002)*, (Dubrovnik, Croatia), 2002.
- [6] S. Ryvkin, *Sliding Mode Control of Synchronous Motor Drive*. Moscow, Russia: Nauka Academic Publishing House, 2009. In Russian.
- [7] V. I. Utkin, J. Güldner, and J. Shi, *Sliding Mode Control in Electromechanical Systems*. Oxon, UK: Taylor & Francis Group, 1999.
- [8] A. Šabanović and K. Jezernik, *Variable Structure Systems: from principles to implementation*, ch. Sliding mode in motion control systems, pp. 295–318. IET Control Engineering Series no. 66, The Institution of Engineering and Technology, 2004.
- [9] G. S. Buja and M. P. Kazmierkowski, "Direct torque control of PWM inverter-fed ac motor – a survey," *IEEE Transactions on Industrial Electronics*, vol. 51, no. 4, pp. 744–757, 2004.
- [10] C. Lascu, I. Boldea, and F. Blaabjerg, "Variable-structure direct torque control – a class of fast and robust controllers for induction machine drive," *IEEE Transactions on Industrial Electronics*, vol. 51, no. 4, pp. 785–792, 2004.
- [11] J. Vittek, S. J. Dodds, P. Bris, M. Stulrajter, and P. Makys, "Experimental verification of chattering-free sliding mode control of the drive position employing PMSM," *Journal of Electrical Engineering*, vol. 59, no. 3, pp. 139–145, 2008.
- [12] S. Ryvkin, R. Schmidt-Obermoeller, and A. Steimel, "Sliding-mode-based control for a three-level inverter drive," *IEEE Transactions on Industrial Electronics*, vol. 55, no. 11, pp. 3828–3835, 2008.
- [13] W. Leonhard, *Control of Electrical Drives*. Berlin, Germany: Springer Verlag, 3rd ed., 2001.
- [14] A. N. ande I. Takahashi and H. Akagi, "A new neutral-point-clamped PWM inverter," *IEEE Transactions on Industrial Applications*, vol. 17, no. 5, pp. 518–523, 1981.



Sergey Ryvkin was born in Moscow, Russia in 1951. He graduated from Moscow Institute for Aviation Engineering (Dipl.-Eng.), Moscow, USSR, in 1974 and received the Ph.D degree in control and electrical drive from the Institute of Control Sciences of Russian Academy of Sciences, Moscow, USSR, in 1986 and the Dr. Sci. (Eng.) in control from the Supreme Certifying Commission of Ministry of Education and Science, Moscow, Russia, in 2006. From 1974 to 1977 he was with the Drive Division of Moscow plant "Dserzhinec". Since 1977 till today he works in the Institute of Control Sciences, now as Leading Researcher. In 1999-2003 he worked as a part time Professor at National Textile University, Moscow, Russia and since 2006 he is a part-time Professor at the Russian State University for the Humanities, Moscow, Russia. His research interests are in variable structure systems with sliding mode as applied to power electronics system, multilevel converters and high dynamic electrical drives control. Prof. Ryvkin is a Full Member of the Russian Academy of Electrotechnical Sciences, a Corresponding Member of the EPE-PEMC Council, a Vice-Chair of Joint Chapter PELS/IES/PES/IAS of Russian Section and a member of the Board of Editors of the leading Russian electrotechnical journal "Elektrichestvo". Since 1986 he was in charge of the industrial projects between his Institute and different large Russian companies. He was granted MacArthur Foundation as an individual research (January 1994 to June 1995), German Academic Exchange Service as a visiting research (November 2006 to January 2007), Russian Foundation for Basic Research (2008) as a scientific book writer. He has published one monograph (2009), three textbooks, more than 100 technical papers in international journals and conferences and has 6 invention certificates.

AUTHORS' ADDRESSES

Prof. Sergey Ryvkin, Ph.D.
Trapeznikov Institute of Control Sciences,
Russian Academy of Sciences,
Profsoyuznaya ul. 65, 117997, Moscow, Russia
email: rivkin@ipu.rssi.ru

Received: 2010-03-13

Accepted: 2010-04-09